Microwave Phase Shift Using Ferrite–Filled Waveguide Below Cutoff

CHARLES R. BOYD, JR.

Microwave Applications Group, Santa Maria, California, U. S. A.

ABSTRACT

Unlike conventional waveguides, lossless ferrite–filled guides may exhibit a complex propagation factor below cutoff of the dominant TE mode when a transverse magnetic bias field is applied. In that case, the field in a very long waveguide has the character of a traveling wave whose amplitude decays exponentially with distance from the driven end. The wavelength and the magnitude of the applied bias field are inversely related, and at zero field as the gyromagnetic effects vanish in the ferrite the wavelength becomes infinite. For a bias field of one polarity, the traveling wave will be a forward wave, and for the opposite polarity a backward wave.

This peculiar behavior allows phase shift to be produced in a band pass filter–like structure in which small cross–section, below–cutoff ferrite waveguide sections alternate with sections of high dielectric constant material.

I. INTRODUCTION

Some years ago, the author presented an analysis of differential phase for the dominant TE mode in completely filled circular ferrite waveguide with transverse fourpole magnetic bias[1]. In that paper it was noted that the amount of differential phase did not depend on the dielectric constant of the ferrite material. What was not commented upon, but is obvious from inspection of the equations, is that the amount of differential phase also does not depend upon whether the frequency is above or below the dominant TE mode cutoff frequency. This analysis was based on a simplified transmission–line model for the lossless nonreciprocal ferrite–loaded waveguide, which was eventually also published[2].

More recently, the search for ways to reduce the size of rotary–field ferrite phase shifters led to configurations in which sections of ferrite waveguide alternate with sections of nonmagnetic ceramic material of much higher dielectric constant[3]. The cross–sectional dimensions of this filter–like structure may then be reduced to a fraction of the diameter needed to propagate in a uniform ferrite rod. In carrying out this development it was assumed, and verified experimentally, that the differential phase calculated using [1] was valid, even though the ferrite waveguide sections could be below cutoff at the operating frequency.

Such behavior implies that waves of bias–field–adjustable wavelength exist in the cutoff ferrite waveguide, a condition that contrasts sharply with the case of an ordinary lossless waveguide below cutoff. In that case the propagation factor is pure real, indicating that the incident and reflected fields have constant phase and decay exponentially in the guide. The total field may exhibit a phase difference across a lossless section of ordinary cutoff waveguide because of the end conditions, however.

This paper examines the solutions for propagation factor in a lossless ferrite waveguide biased with a transverse magnetic field and operated at a frequency below cutoff of the dominant TE mode. The analysis is based on the approach of [2]. The peculiar characteristics observed above turn out to be predicted (but strange) results of the analysis.

II. ANALYTICAL MODEL

For time–harmonic electromagnetic fields in uniform cylindrical waveguides, it is customary to separate the transverse distribution of the fields from the variation along the axis of the guide. Using the notation of Harrington[4], normalized transverse field vector mode functions $\mathbf{e}(x,y)$ and $\mathbf{h}(x,y)$ may be defined, with the normalization such that the squared magnitudes of these functions integrate to unity over the transverse plane. All amplitude factors are then expressed in a z–dependent mode "voltage" $V(z)$ and mode "current" $I(z)$, and the transverse fields $\mathbf{E}_t$ and $\mathbf{H}_t$ are given by

$$\mathbf{E}_t = \mathbf{e}(x,y)\, V(z) \; , \qquad \mathbf{H}_t = \mathbf{h}(x,y)\, I(z) \qquad (1)$$

Determining the transverse field distribution then involves the solution of a two–dimensional Helmholtz–equation boundary value problem, while the longitudinal variations of the scalar amplitudes V and I behave according to the elementary transmission line equations. In cases where a detailed knowledge of the transverse field distribution is not required, it is sometimes possible to replace the actual waveguide field problem by an equivalent transmission–line problem using distributed lumped–element parameters. Proper implementation of this approach easily yields the propagation factor for the waveguide.

As an example, consider the familiar transmission–line representation for the dominant TE_{10} mode in a uniform, homogeneously filled ordinary rectangular waveguide, shown in Figure 1. When the distributed series inductance and
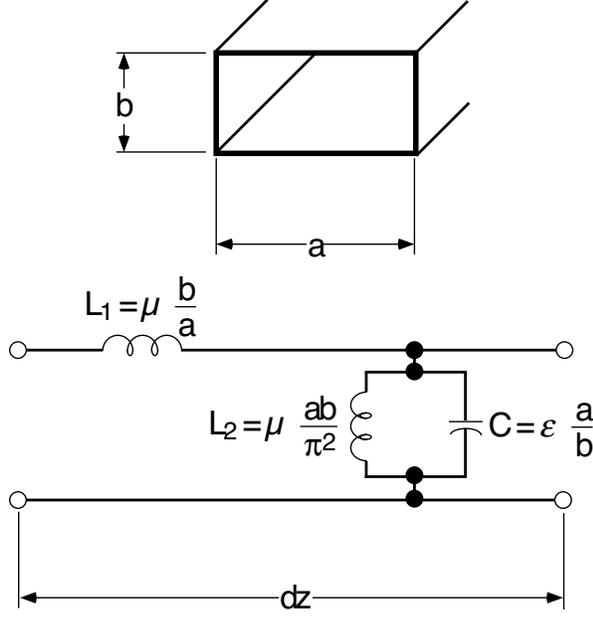
Fig. 1 Rectangular waveguide and transmission–line equivalent model for TE_{10} mode.

parallel shunt LC elements are defined as shown, the propagation factor readily computes to

$$\gamma = \pm \sqrt{ZY} = \pm j\,\beta_0 \sqrt{1 - \left(\frac{\omega_c}{\omega}\right)^2} \qquad (2)$$

where $\beta_0 = \omega\sqrt{\mu\varepsilon}$ is the free space propagation factor in the medium filling the waveguide, and $\omega_c = \frac{\pi}{a}\frac{1}{\sqrt{\mu\varepsilon}}$ is the cutoff frequency of the mode. Note that the series and shunt inductances can be combined into a diagonal matrix **L** as follows:

$$\mathbf{L} = \frac{L_1}{k_c}\begin{bmatrix} k_c & 0 \\ 0 & \frac{1}{k_c} \end{bmatrix} \qquad (3)$$

Here $k_c = \frac{\pi}{a}$ is the cutoff wave number for the rectangular waveguide dominant mode. With the inductances combined in this form, it is easy to generalize the transmission–line model to guides with other relationships for k_c, and to include a distributed gyrator that couples the series and shunt members. The extended model is shown in Figure 2. Nonreciprocal coupling between the series and shunt inductances is the network equivalent of similar coupling between the transverse and longitudinal magnetic fields of the waveguide TE mode. Following [2], the inductance matrix for the coupled case becomes

$$\mathbf{L} = \frac{L_1}{k_c(1 - \zeta^2)}\begin{bmatrix} k_c & -j\,\zeta \\ j\,\zeta & \frac{1}{k_c} \end{bmatrix} \qquad (4)$$

where the coupling factor ζ depends on the extent p to which
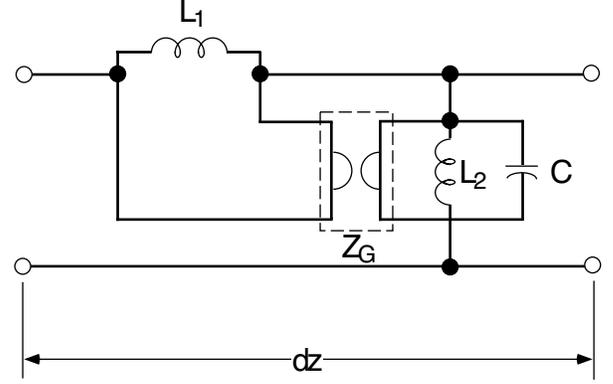
Fig. 2 Extended transmission–line equivalent model incorporating a distributed gyrator.

the geometry and bias field configuration favors nonreciprocal effects, as well as on the permeability tensor element values produced in the ferrite by the transverse magnetic bias field, i. e.

$$\zeta = p\,\frac{\kappa}{\mu} \qquad (5)$$

A rationale for the parallel connection of distributed inductor and gyrator elements in the equivalent circuit has been presented previously[5]. Essentially, the μ factor of the inductance L_1 is implicitly dependent on the permeability tensor of the magnetized ferrite. For a guide completely filled with uniformly magnetized ferrite and no gyrator coupling, μ will be replaced by μ_{eff}, given by

$$\mu_{eff} = \frac{\mu^2 - \kappa^2}{\mu} = \mu\left[1 - \left(\frac{\kappa}{\mu}\right)^2\right] \qquad (6)$$

With parallel gyrator coupling, the determinant $1 - \zeta^2$ of the inverse of the **L** matrix appears as a denominator multiplying L_1, so that for the case being considered, the net result is an equivalent μ factor for L_1 of the form,

$$\mu_{equiv} = \mu\,\frac{1 - \left(\frac{\kappa}{\mu}\right)^2}{1 - \left(p\,\frac{\kappa}{\mu}\right)^2} \qquad (7)$$

and for p varying from zero to unity the value for μ_{equiv} transitions smoothly from μ_{eff} to the diagonal element μ of the permeability tensor. This is an important behavior for Faraday rotators, although for the single–mode guide of interest here, the net effect is a slight shift in the guide cutoff frequency.

The propagation factor for the extended transmission–line model may now be determined by assuming solutions for the voltage and current quantities that vary as $\exp(\gamma z)$ and finding the roots of the characteristic equation:

$$\gamma = -j\left[k_c\,\zeta \pm \omega\sqrt{L_1 C}\,\sqrt{1 - \left(\frac{\omega_c}{\omega}\right)^2(1 - \zeta^2)}\,\right] \qquad (8)$$

Defining the initial ($\zeta = 0$) infinite–medium propagation factor as $\beta_0 = \omega\sqrt{L_1 C}$, equation (8) can be written in the form

$$\gamma = j\,\beta_0\left[\,\zeta\left(\tfrac{\omega_c}{\omega}\right)\pm\sqrt{1-\left(\tfrac{\omega_c}{\omega}\right)^2(1-\zeta^2)}\,\right] \qquad (9)$$

Evidently equation (9) reduces to the ordinary waveguide case of equation (2) when the nonreciprocal coupling ζ vanishes. The square–root term of equation (9) expresses the ordinary bidirectional waveguide propagation, which has a second–order symmetric modification of cutoff frequency because of the nonreciprocal coupling. In most practical cases of interest this shift should be small. The first term gives the main effect of the nonreciprocal coupling, which is independent of the direction of propagation. When the frequency is far above cutoff, this term will add numerically to the propagation factor in one direction of propagation and subtract from it in the other direction. Since the sign of ζ changes with the direction of the magnetic bias field, the net propagation factor will move up and down antireciprocally from the ordinary waveguide value as the magnetic bias field is varied from its maximum negative to maximum positive value.

The characteristic impedances associated with the propagation factors turn out to be numerically equal, and are given by[2]

$$Z_0 = \sqrt{\dfrac{L_1}{C\left[1-\left(\tfrac{\omega_c}{\omega}\right)^2(1-\zeta^2)\right]}} \qquad (10)$$

III. CONDITIONS BELOW CUTOFF

Cutoff occurs when the term under the radical in equation (9) vanishes. For frequencies below the cutoff value, equation (9) is properly rewritten as

$$\gamma = j\,\beta_0\,\zeta\left(\tfrac{\omega_c}{\omega}\right)\pm\beta_0\sqrt{\left(\tfrac{\omega_c}{\omega}\right)^2(1-\zeta^2)-1} \qquad (11)$$

and by defining

$$\alpha \equiv \beta_0\sqrt{\left(\tfrac{\omega_c}{\omega}\right)^2(1-\zeta^2)-1} \qquad (12)$$

the propagation factor takes on the form of an attenuated wave. That is, for a waveguide driven at one end and extending to infinite z, the field quantities will vary along the guide as

$$V(z) = V_0\,e^{\pm\alpha z}\,e^{j\beta_0\zeta\left(\tfrac{\omega_c}{\omega}\right)z} \qquad (13)$$

with the two choices of sign of αz corresponding with the two cases in which the field value for an infinitely long guide vanishes at either positive or negative infinity. The nonreciprocal coupling still produces a traveling wave, now attenuated, that moves in a direction determined only by the direction of the magnetic bias field. For one bias field direction the waves will travel away from the driven end, and for the other bias field direction the waves will travel toward the driven end. The characteristic impedances of the two roots will both be purely imaginary, and again numerically equal:
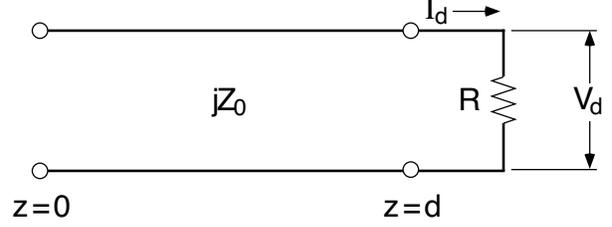
Fig. 3 Model for short ferrite waveguide below cutoff.

$$jZ_0 = j\sqrt{\dfrac{L_1}{C\left[\left(\tfrac{\omega_c}{\omega}\right)^2(1-\zeta^2)-1\right]}} \qquad (14)$$

As in a guide above cutoff, the characteristic impedance expresses the relationship between the normal–mode line voltage and current. The imaginary value of characteristic impedance for the below–cutoff case simply expresses the fact that the normal–mode voltage and current have a specific amplitude ratio but are in time quadrature. Because the direction of the current flow is opposite between the mode attenuating in the positive–z direction and the mode attenuating in the negative–z direction, the quadrature relationship will be reversed for one mode relative to the other. These conditions are analogous to the propagating case, and permit the voltage–current relationship to be satisfied for arbitrary end conditions in a guide of finite length.

IV. END CONDITIONS FOR A WAVEGUIDE BELOW CUTOFF

Consider now the case of Figure 3, in which a short length d of cutoff ferrite waveguide is terminated in a resistive load R. Solutions of the transmission line equations for this case give the following for V(z) and I(z):

$$V(z) = V_d\left\{\cosh[\alpha(z{-}d)]-j\tfrac{Z_0}{R}\sinh[\alpha(z{-}d)]\right\}e^{-j\beta(z-d)}$$

$$I(z) = \tfrac{V_d}{R}\left\{\cosh[\alpha(z{-}d)]+j\tfrac{R}{Z_0}\sinh[\alpha(z{-}d)]\right\}e^{-j\beta(z-d)} \qquad (15)$$

Here β stands for the imaginary part of γ in equation (11). Note that the power flow in the cutoff guide meets the necessary criterion, i. e.

$$P = Re\left\{V(z)I^*(z)\right\}$$
$$= \tfrac{V_d^2}{R}\left\{\cosh^2[\alpha(z{-}d)]-\sinh^2[\alpha(z{-}d)]\right\}=\tfrac{V_d^2}{R} \qquad (16)$$

Clearly, the expressions above involve both normal modes, with fields decaying in positive and negative z, respectively. For a better insight, it is useful to think of the positive–z decaying mode as the incident field and the negative–z decaying mode as the reflected field, much as the above–cutoff case considers end conditions in terms of incident and reflected traveling waves. Then the reflected and incident fields can be related through a load–dependent reflection coefficient. The diagrams of Figure 4 show the combination of incident and
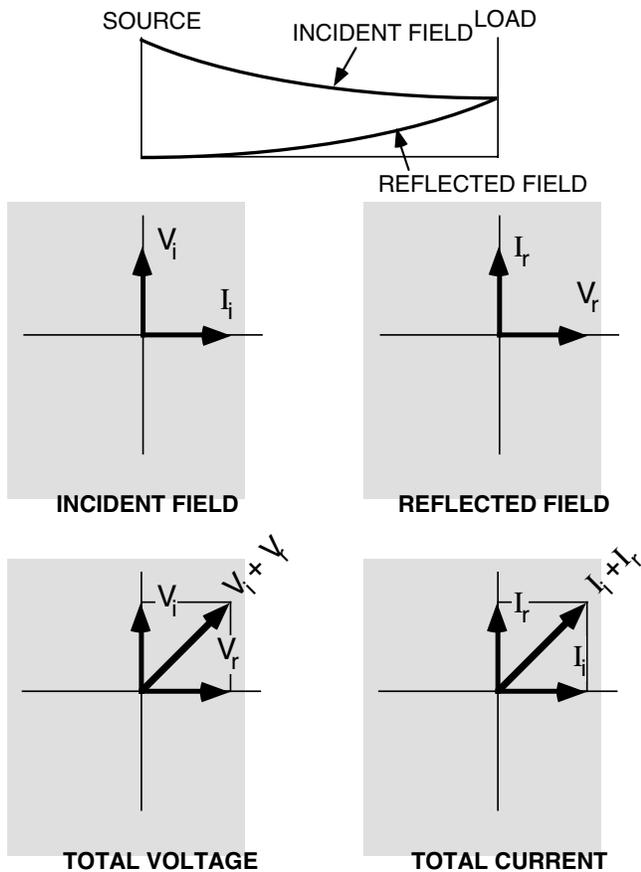
Fig. 4 Incident and reflected field conditions for termination in a real load of $R = |Z_0|$.

reflected field phasors that will exist at the end of a long cutoff section terminated in a real load whose resistance is equal to the magnitude of the characteristic impedance of the cutoff guide. For this case the phase of the voltage across the load differs from the phase of the incident field by 45 degrees. For other values of load resistance or for shorter sections of cutoff guide, the phase will generally differ from 45 degrees but will be in the range of zero to 90 degrees relative to the phase of the incident field.

Note that the magnitudes of the incident and reflected fields are equal at the termination, i. e. the reflection coefficient has a magnitude of unity. This is a general condition that applies whenever a cutoff guide terminates into a pure real load, as can be seen by forming the squared magnitude of the reflection coefficient:

$$|\rho|^2 = \left|\frac{R - jZ_0}{R + jZ_0}\right|^2 = 1 \tag{17}$$

Evidently a duality of sorts exists between the cutoff guide and the propagating guide, since terminating a guide with real Z_0 into a pure reactance also yields unity magnitude of reflection coefficient. To achieve zero reflected field, a cutoff guide

may be terminated in a pure reactance equal to the characteristic impedance of the guide. Because it is possible to terminate the cutoff guide in a reactance of the opposite sign from the characteristic impedance, the reflected field may be greater than the incident field. In fact, terminating a cutoff guide in a lossless system into the complex conjugate reactance of the characteristic impedance causes a singularity in the reflection coefficient, i. e. the entire structure resonates with infinite Q. Obviously the inherant losses in a practical structure will limit the ratio between magnitudes of the incident and reflected fields to a finite value.

The familiar Smith Chart presents a useful mapping relationship between the normalized load of a guide with real Z_0 and the resulting reflection coefficient. An analogous presentation can be made for the case of a terminated below–cutoff guide, as shown in Figure 5. For a cutoff waveguide, the right half of the impedance (or admittance) plane maps into two half–Smith Charts, one based on $|\rho|$ as the distance from $X/Z_0 = 1$, the other based on $1/|\rho|$ as the distance from $X/Z_0 = -1$. The unit half–circles of each chart represent the same conditions of termination in positive real load impedance.
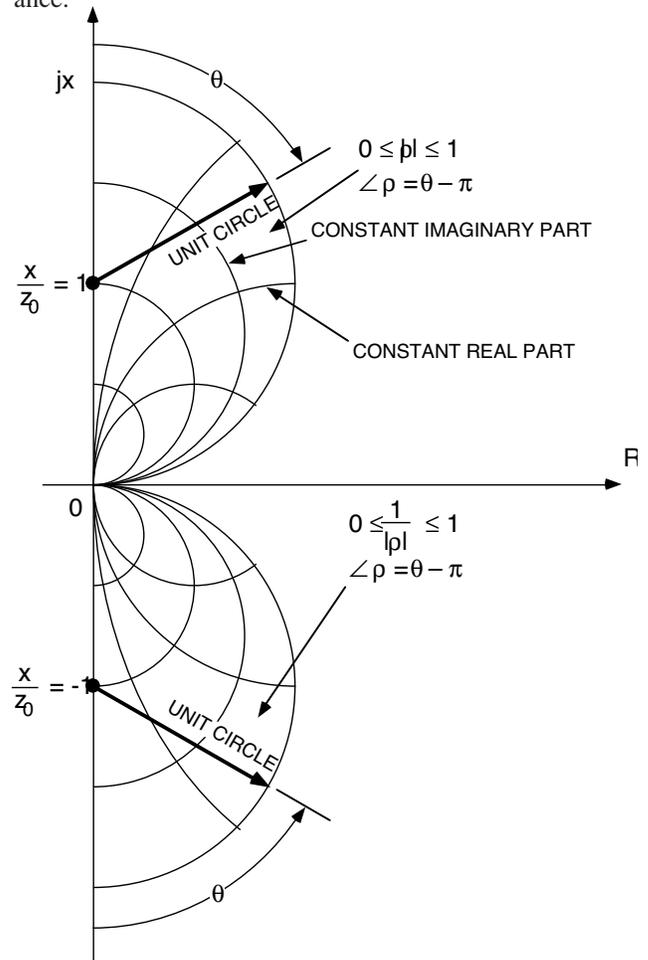
Fig. 5 "Smith Chart" for reflections at the end of a cutoff guide.

V. PERIODICALLY LOADED GUIDE

Next, consider a lossless filter–like structure that is comprised of short lengths 2d of cutoff ferrite waveguide alternating with generally different short lengths of guide filled with a material of much higher dielectric constant. If the frequency and physical parameters are chosen such that the composite structure is near the center of a pass band, and if R is taken as the load at the end of a terminating ferrite guide half–section of length d, then the impedance level at the midpoint of each ferrite section of length 2d will also be equal to R. Inspection of equations (15) for this case reveals that the magnitudes of the voltage and current will be symmetric in z with respect to the midpoint d for each ferrite section. Then the ferrite guide sections will each appear to propagate a bias–field dependant traveling wave whose magnitude is minimum at the center and rises at the ends. Conversely, the high–dielectric sections, which must be above cutoff, propagate a normal wave whose amplitude is maximum at the center of the sections and droops symmetrically toward the ends. Figure 6 shows a plot of the field magnitude levels for a typical case of periodically loaded structure.

FERRITE DIELECTRIC FERRITE DIELECTRIC FERRITE
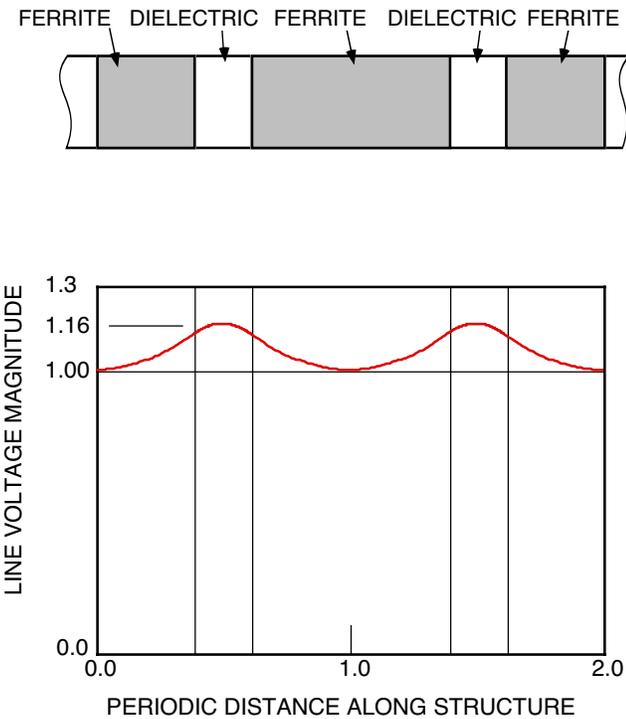
Fig. 6 Field amplitude vs. distance in a typical periodic structure.

As indicated above, the wavelength in the ferrite sections is inversely related to the magnetic bias field level, becoming infinite for zero bias as the gyromagnetic effects in the ferrite vanish. For one polarity of bias field the wave will travel in the same direction as the energy flow, i. e. a forward wave, and for the other polarity of bias field the wave will travel in the opposite direction, i. e. a backward wave.

Since the magnetic bias field may be changed between positive and negative maximum values, the available phase shift $\Delta\phi$ from N cutoff ferrite waveguide sections of cumulative length 2Nd will be, from equation (13),

$$\Delta\phi = 4N\beta_0 d\ p\ \frac{\kappa}{\mu}\ \frac{\omega_c}{\omega} \tag{18}$$

But $2N\beta_0 d$ is the insertion phase for a plane wave propagating through the distance 2Nd in an infinite ferrite medium, which can be defined as ϕ_0 and used as a normalization:

$$\frac{\Delta\phi}{\phi_0} = 2\ p\ \frac{\kappa}{\mu}\ \frac{\omega_c}{\omega} \tag{19}$$

Equation (19) is exactly the same as the result derived for ferrite waveguides *above* cutoff and previously published in reference [1]. In [2] a perturbational method was used to calculate a value of $p = 2/\pi$ for the case of a rectangular waveguide fully filled with ferrite, operating in the dominant TE mode, and with constant magnetic bias in the positive y–direction over one half the cross–section and in the negative y–direction over the other half. For a circular guide completely filled with ferrite and biased by a transverse fourpole magnetic field, a value of $p = 0.615$ has been recommended[1] on the basis of experimental data.

VI. EXPERIMENTAL RESULTS

A test configuration has been built using eleven alternating sections of 800 Gauss garnet material of $\varepsilon \approx 15$ and a nonmagnetic ceramic material of $\varepsilon \approx 100$ in a circular waveguide. The cutoff frequency of the ferrimagnetic guide sections was approximately 3.7 GHz., and the structure was optimized for a pass band from 2.8 to 4.3 GHz., with the band from 3.0 to 3.5 chosen as the target range for impedance matching to a conventional rectangular waveguide at each end. At 3.0 GHz. the estimated maximum value for ζ is 0.28. Figure 7 shows a photograph of the test structure prior to metallization, and Figure 8 shows the computed return loss of the configuration
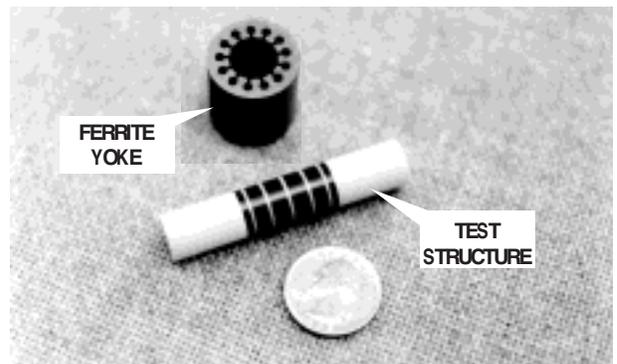
Fig. 7 Unmetallized test structure showing alternating sections.

over the optimized pass band. A close fitting ferrite yoke was placed over the garnet–ceramic rod and the phase shift available for a linearly polarized wave in the structure was measured as a function of the transverse fourpole magnetic bias field drive, producing the "hysteresis loop" shown in Figure 9.

VII. Conclusions

Phase shift is not only possible in below–cutoff ferrite waveguides, but the phase shift per unit length actually increases as the diameter of the guide is reduced. Alternating short sections of cutoff ferrite guide with sections of nonmagnetic ceramic materials of high dielectric constant allows small rotary–field phase shifters to be built retaining the superior control and phase accuracy of that class of device. As the size and weight of the units is decreased, the peak and average power handling capability will decrease, and the insertion loss will increase. However, the increase of insertion loss is with reference to a very low base level because the amount of ferrite required for a rotary–field phase shifter is only enough to produce a differential phase of 180 degrees.

VII. References

[1] C. R. Boyd, Jr.,"Design of ferrite differential phase shift sections," *1975 IEEE MTT–S Int'l Symposium Digest*, pp. 240–242, May 1975.

[2] C. R. Boyd, Jr.,"A transmission line model for the lossless ferrite–loaded nonreciprocal waveguide," *Proc. Int'l Symposium on Microwave Tech. in Industrial Development–Brazil*, pp. 209–216, July 1985.

[3] C. R. Boyd, Jr. and C. M. Oness, "Ferrite rotary–field phase shifters with reduced cross–section," *1990 IEEE Int'l Microwave Symposium Digest*, pp. 1003–1006, May 1990.

[4] R. F. Harrington,"Time–Harmonic Electromagnetic Fields", Chapter 8, McGraw–Hill Book Co., 1961.

[5] C. R. Boyd, "A network model for transmission lines with gyromagnetic coupling", *IEEE Trans on Microwave Theory Tech.*, vol. MTT–13, pp. 652–662, Sept. 1965.
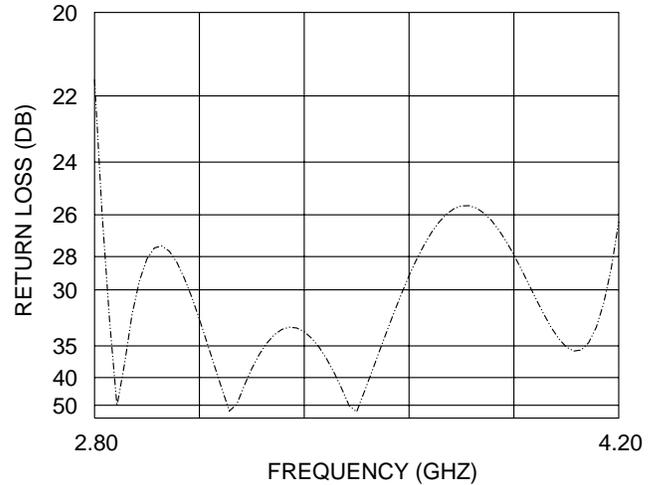
Fig. 8 Computed return loss for test structure.
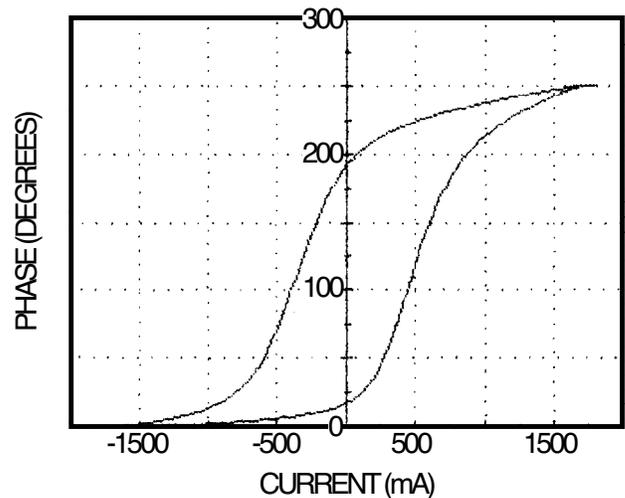
Fig. 9 Microwave phase versus magnetic bias field drive.